J Mater Sci (2008) 43:3917–3922
DOI 10.1007/s10853-007-2401-4

TEM and HAADF-STEM study of the structure of Au nano-particles on CeO_2

Tomoki Akita · Koji Tanaka · Masanori Kohyama

Received: 1 August 2007 / Accepted: 12 December 2007 / Published online: 21 March 2008

Abstract The structure and growth process of Au particles on CeO_2 were observed by the transmission electron microscope (TEM) equipped with the high-angle annular dark-field scanning transmission electron microscopy (HAADF-STEM) system. The growth of Au particles on CeO_2 was shown to be mainly Ostwald ripening under heating at various temperatures, although it is suppressed in the hydrogen atmosphere. In the HAADF-STEM observation of Au/CeO_2 interfaces with the orientation relationship of (111)[1–10]Au//(111)[1–10]CeO_2, (111)[−110]Au//(111)[1–10]CeO_2 and atomic columns of Au and Ce were successfully resolved, and the interface structure was analyzed in details for the first time.

Introduction

It is well known that Au nano-particles supported on metal oxides exhibit high catalytic activity [1]. The catalytic properties are sensitive to the size of Au particles, the kind of metal oxide support and the interface structure between Au particles and metal oxide support. Some experimental results indicate that the perimeter of Au particles on metal oxide surfaces plays a key role in the low-temperature CO oxidation [2, 3]. The understanding of the details of atomic and electronic structures of Au/oxide interface systems is crucial to elucidate the mechanism of the catalytic activity, although this is not yet attained. Recently, Au particles supported on CeO_2 (fluorite structure, space group: Fm3m, lattice constant $a = 0.541134$) catalysts are widely studied because the Au/CeO_2 catalysts show high catalytic activity for low-temperature water–gas shift reaction or CO oxidation [4, 5]. The atomic and electronic structures of Au particles on CeO_2 were investigated by various techniques such as X-ray diffraction (XRD), X-ray photoelectron spectroscopy (XPS), Fourier transform infrared (FT-IR) spectroscopy, etc. [6–8]. However, it is important to apply recent techniques of the electron microscope so as to clarify the structures of Au particles and Au/CeO_2 interfaces in atomic scale.

In this article, transmission electron microscopy (TEM) and high-angle annular dark-field-scanning transmission electron microscopy (HAADF-STEM) observations are applied to the Au/CeO_2 systems. The HAADF-STEM observation has the advantage that atomic columns are directly identified, when the small electron probe and sufficient collection angle for annular detector [9, 10], while complicated simulations of images are needed for the analysis of conventional TEM images, and the HAADF-STEM has been successfully applied to grain boundaries or interfaces in various materials [11, 12]. In this article, we have obtained HAADF-STEM images of the Au/CeO_2 interfaces with the atomic resolution for the first time, and the interface structures are analyzed.

On the other hand, in order to control the size and distribution of Au particles on CeO_2 which have significant effects on the catalytic activity, it is crucial to understand the growth mechanism of Au particles on CeO_2. In our previous TEM observations of Au/CeO_2 catalysts, we found the dynamical and reversible structural changes of Au particles according to the O-vacancy formation and recovery in CeO_2 or the reduction and oxidation of CeO_2 [13, 14]. The following in situ high-temperature TEM

T. Akita (✉) · K. Tanaka · M. Kohyama
Research Institute for Ubiquitous Energy Devices, National Institute of Advanced Industrial Science and Technology (AIST), Midorigaoka 1-8-31, Ikeda, Osaka 563-8577, Japan
e-mail: t-akita@aist.go.jp

observation on the structural changes of Au particles [14] has also indicated the importance of the CeO_2 surface or bulk states such as the density of O vacancies or the oxidization state. In this article, we also perform ex situ TEM observations of the changes of Au particles under heating at various temperatures both in air and in the hydrogen stream, which should provide additional insights into the mechanism of the structural changes or growth of Au particles on CeO_2. The interface atomic structure is also closely involved in this problem.

Experimental

Au nano-particles are deposited on CeO_2 substrate as explained in our previous report [13]. Poly-crystalline CeO_2 was made from the tablet of CeO_2 by heating at 1,673–1,873 K for 10 h in air. The poly-crystalline CeO_2 was cut in 3-mm disk, and the center part was thinned by a mechanical polish and Ar ion beam milling for TEM observation. The CeO_2 substrate was heated at 873 K for 4 h in air, so as to remove the damages by mechanical polish and ion beam irradiation. Au particles were deposited by vacuum deposition. An Au wire with 0.2 mm in diameter attached to the tungsten basket was heated in vacuum chamber. The amount of Au was controlled by the length of the Au wire. The vacuum deposition was carried out under 10^{-6} Torr. Carbon contaminants during the sample preparation process were removed by heating treatment. The samples were heated in air and in reductive atmosphere. For the reductive heating, the samples are heated in the hydrogen stream diluted by Ar (Ar: $H_2 = 8{:}2$) with a flow rate of 33 mL/min. The TEM and HAADF-STEM observations were carried out by using JEOL JEM-3000F transmission electron microscope (TEM) equipped with digitally processed STEM imaging system. The TEM observation was done for the same area after each heating treatment via the transfer from TEM to a furnace or a glass vessel. The size distribution measurement of Au particles was carried out by using the image analysis software Image-Pro for the digitally processed TEM images. The size of Au particle was defined as the average of maximum diameter and minimum diameter for the particles, which is not complete spherical shape.

Results and discussion

Figure 1 shows TEM images and size distribution of Au particles heated in air for 4 h at temperatures, 473, 573, 673, and 873 K, respectively. The TEM images were obtained sequentially from the same area after each heating treatment, so as to clarify the growth process of Au particles. The TEM images were taken with the off-Bragg

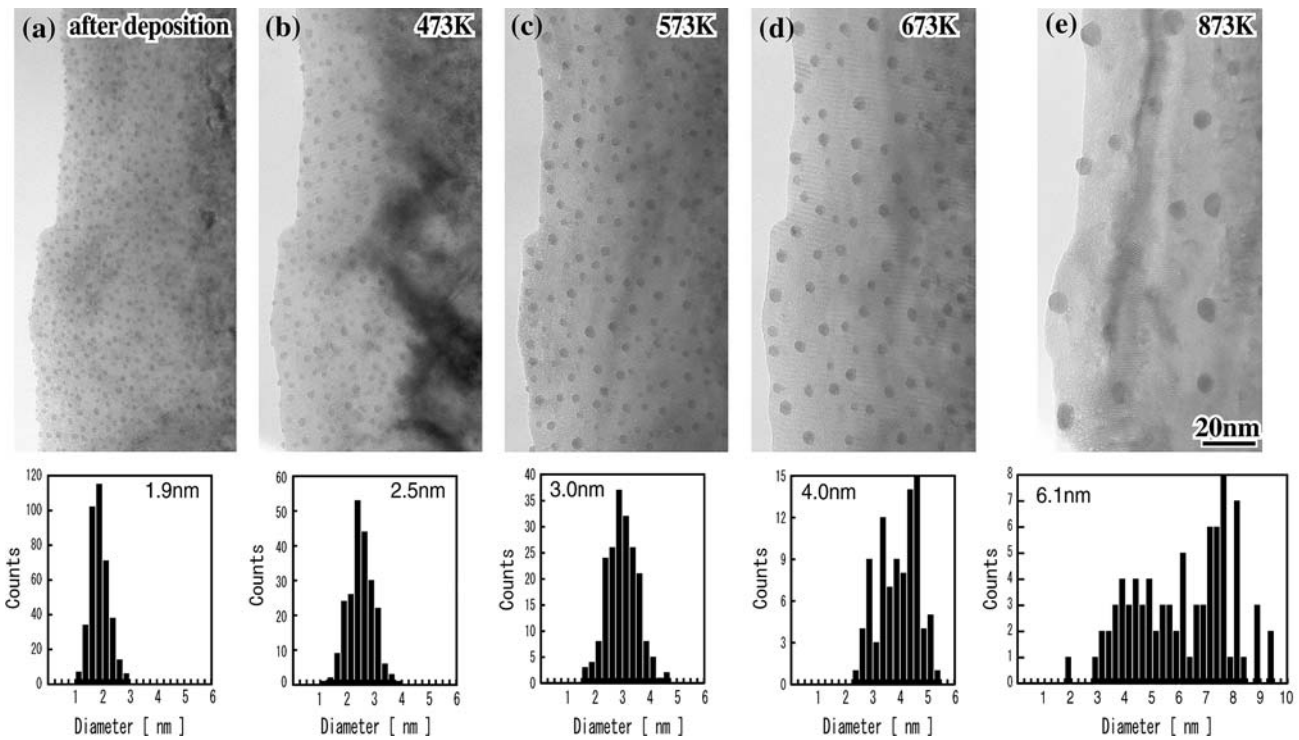

Fig. 1 TEM images of Au particles on CeO_2 and size distribution of Au particles. The images are taken after deposition (**a**) and after heating in air at 473 K (**b**), 573 K (**c**), 673 K (**d**) and 873 K (**e**)

condition for the CeO_2 crystal in order to obtain enough contrast for small Au particles, which are observed as dark particles. In the sequential TEM images, the Au particles grow by heating, and the mean diameter of Au particles changes from 1.9 to 6.1 nm. It is noteworthy that the position of each Au particle is not changing. Small Au particles disappear by heating and large Au particles grow larger. This growth process means Ostwald ripening, which is characterized by the formation of larger Au particles at the expense of smaller Au particles, as observed in situ heating TEM observation of Au particles on CeO_2 [15].

The Au/CeO_2 samples were also heated in the hydrogen stream. Figure 2 shows the TEM images and size distribution of Au particles heated for 4 h in the hydrogen stream at temperatures from 473 to 673 K. The particle size of Au is not increasing in contrast to the Au particles heated in air. The growth of Au particles is apparently suppressed in the hydrogen atmosphere. The changes of the mean diameter of Au particles heated in air and hydrogen atmosphere are summarized in Fig. 3. It seems that the oxygen vacancies are created on the CeO_2 surface as observed by scanning tunnelling microscopy (STM) in ultra-high vacuum condition [16] and prevent the diffusion of Au atoms on the CeO_2 surface in the hydrogen stream [8], considering that the reduction of the CeO_2 surface occurs at around 373 K when the noble metal particles are supported [4, 17]. The growth of Au particles on TiO_2 is observed for the powder catalysts heated in various conditions, and it is also reported that the growth of Au particles is suppressed in the hydrogen atmosphere [18] by the strong binding energy between an Au atom and the surface O vacancy [19]. These points are practically important to prepare the catalysts with highly dispersed small Au particles.

A high-resolution TEM (HRTEM) image of an Au particle on CeO_2 heated in air at 573 K is presented in Fig. 4. Au particles in this sample are fcc single crystals and have polygonal shapes frequently surrounded by low index facets of (111) and (100). These features of Au particles are common to the samples heated at different temperatures in spite of the different mean sizes of Au particles. The lattice fringes of both the Au particle and CeO_2 support are clearly observed because the incident electron beam is simultaneously aligned along the zone

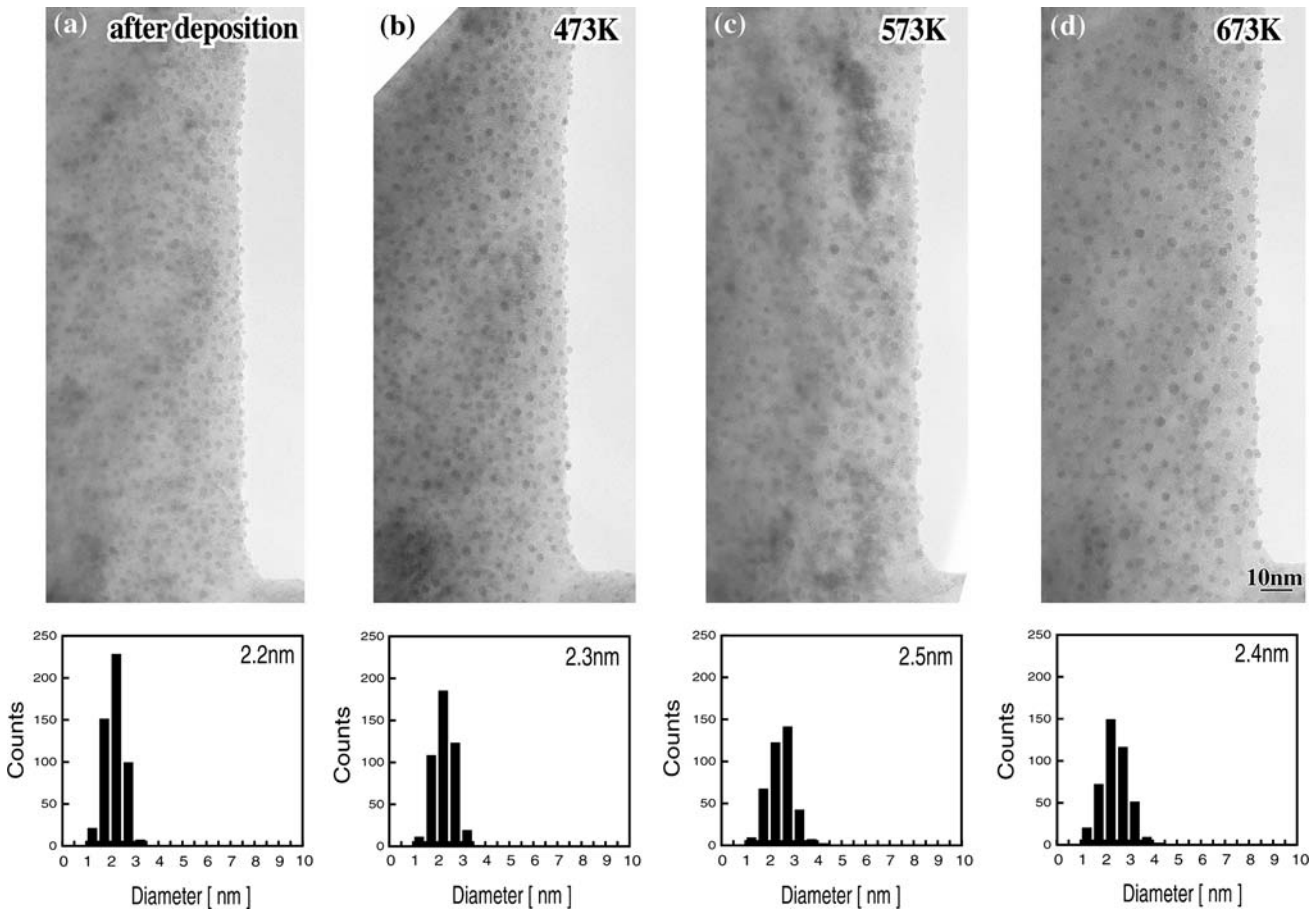

Fig. 2 TEM images of Au particles on CeO_2 and size distribution of Au particles. The images are taken after deposition (**a**) and after heating in H_2 stream at 473 K (**b**), 573 K (**c**) and 673 K (**d**)

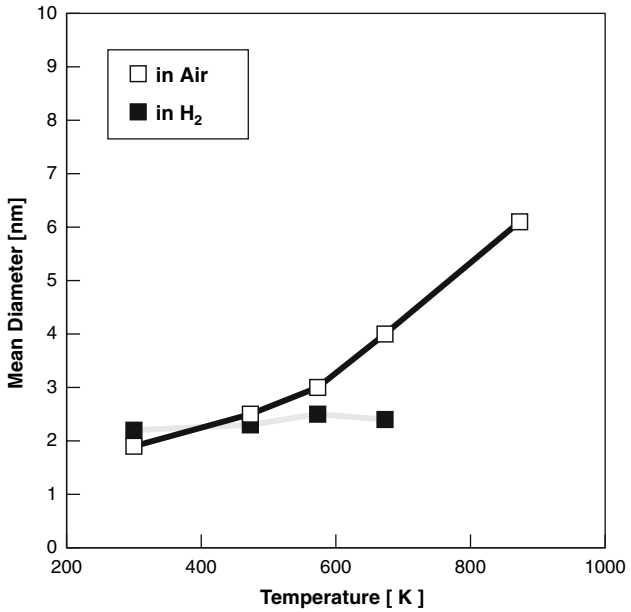

Fig. 3 The mean diameter of Au particles on CeO_2 for sequential heating with increasing temperature in air and H_2 stream

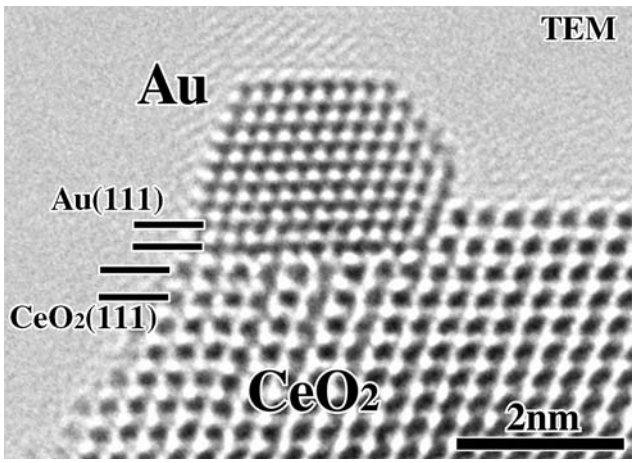

Fig. 4 Profile-view high resolution TEM image of an Au particle on CeO_2

axes of Au[1–10] and CeO_2[1–10]. This means the presence of the special orientation relationship of (111)[1–10]Au//(111)[1–10]CeO_2. This preferential orientation relationship is frequently observed in such profile-view TEM images, as previously reported for the Au particles supported on CeO_2 by the deposition precipitation method [13]. In Fig. 4, an atomic step of the CeO_2(111) surface is observed at the right side of the Au particle. Au particles seem to be stabilized at the edge of atomic steps as observed by STM [8].

No obvious differences in the interface structures are observed in HRTEM images for the samples heated in air and hydrogen stream. This may be because the samples are transferred from heating apparatus to electron microscope through air. CeO_2 is easily oxidized by exposure to air. The structure change of Au particles easily occurs by the reduction and oxidation of CeO_2 surfaces [13, 14]. The detailed differences of the interface structure must be observed by in-situ TEM observation with controlling the heating atmosphere in the chamber.

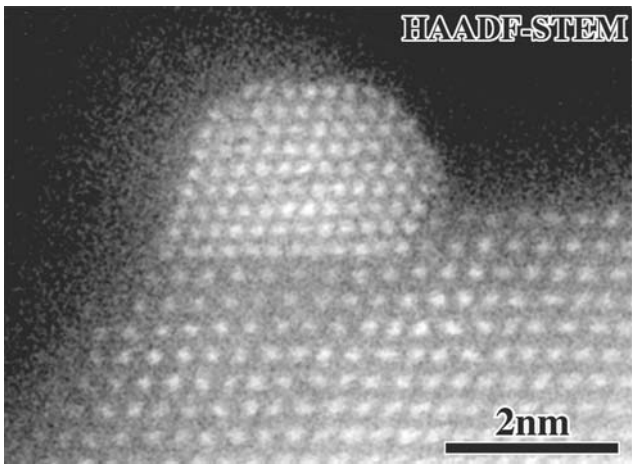

Fig. 5 HAADF-STEM image of the same Au particle on CeO_2 with Fig. 4

The HAADF-STEM image of the interface between Au and CeO_2 is shown in Fig. 5. This was obtained from the same Au particle observed in the TEM image of Fig. 4. The image was recorded with the size of 512 × 512 pixels, the scan speed of 31.5 μs/pixel, and the total acquisition time of 8.2 s. The noise in the image was reduced by smoothing process on the image processing software, Gatan Digital Micrograph. The simple distortion of the image caused by sample drift during image acquisition was corrected manually by using conventional image analysis software. The whole image was expanded for one direction to coincide with the CeO_2 lattice shown in Fig. 4. The position of atomic columns of Au and Ce are clearly resolved as bright contrast in Fig. 5. It is obvious that the atomic positions are easily interpreted by Fig. 5 than by Fig. 4. It is also clear that the Au particle has fcc structure and that a flat (111) face is formed at the Au/CeO_2(111) interface in Fig. 5. Here of course, the HRTEM image (Fig. 4) also contains a lot of information, but the precise simulations are needed to interpret the atomic configurations [20]. The image of the Au particle is not clear at the right side of the particle corresponding to the (100) surface in Fig. 5. This may be explained by the distortion by surface reconstruction of the Au(100) surface. Or this may be caused by the movement of Au atoms during the acquisition of the HAADF-STEM image because the shape of an Au particle changes easily via Au surface diffusion under

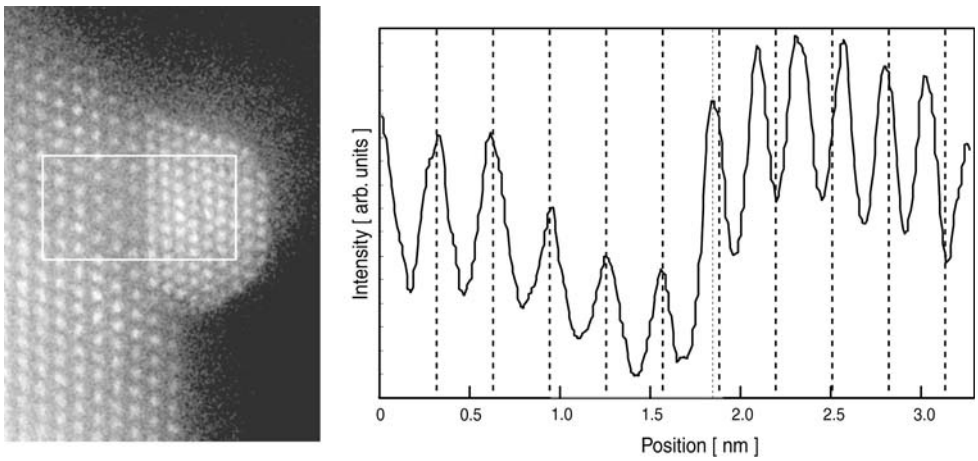

Fig. 6 The intensity profile of the HAADF-STEM image. The intensity is integrated on each plane parallel to the interface in a white rectangle in the left figure, and is plotted normal to the interface

electron beam irradiation [13, 14]. The fluctuation of arrangement of surface atoms were often observed in the TEM observations, the stable situation is just obtained in the TEM image in Fig. 4.

The positions of the Au(111) and Ce(111) atomic layers are estimated from the HAADF-STEM image. The intensity profile of the image is shown in Fig. 6. The intensity integrated parallel to the CeO_2(111) and Au(111) planes inside the white rectangle in the HAADF-STEM image of Fig. 6 is plotted along the normal direction to the interface from CeO_2 region to Au region across the interface. The gradual decrease in the intensity of the CeO_2 side near the interface should be caused by the decrease in the thickness. From the peak positions in the profile, we can determine the positions of each Au(111) and Ce(111) atomic planes and the interface or interlayer distances. The Au(111) interface plane is located on the CeO_2 surface with 0.27 nm from the topmost Ce layer, while the lattice spacing of CeO_2(111) and Au(111) is 0.312 and 0.235 nm, respectively. It is interesting that the interface distance of 0.27 nm is only a little smaller than the average of the interlayer distances of the two crystals. The oxygen columns are not distinguished in the HAADF-STEM images because the intensity of oxygen atoms proportional to the *Z*-number is too weak compared to Au and Ce. No obvious displacements of the atomic columns within the detection limit of the STEM image are observed at the Au/CeO_2 interface in Fig. 5. However, some Au atoms seem to displace slightly, and further discussions are necessary with precise measurements for the HAADF-STEM images, because the specimen drift and fluctuation of a scanning electron beam should distort the STEM images.

Figure 7 shows the HAADF-STEM image of another Au particle. In this case, the orientation relationship of (111)[−110]Au//(111)[1–10]CeO_2 is formed at the Au/CeO_2 interface. This preferential orientation relationship is also sometimes observed for Au particles on CeO_2 [14]. The atomic step of CeO_2 is also observed in the right side

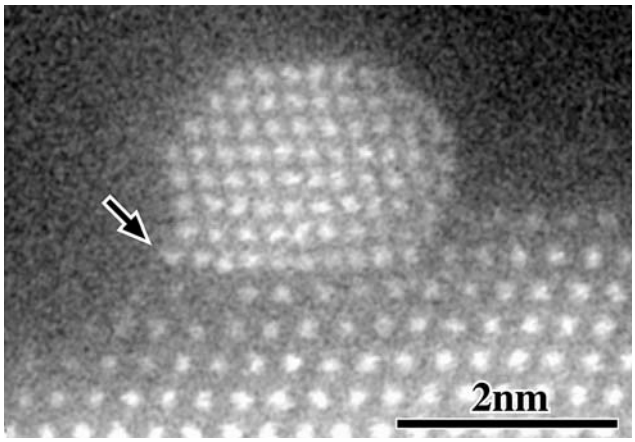

Fig. 7 HAADF-STEM image of an Au particle on CeO_2 with the orientation relationship of (111)[−110]Au//(111)[1–10]CeO_2

of the Au particle. The displacements of atomic columns are observed at the left three columns of the interface Au layer as indicated by an arrow. For these three Au columns, the whole Au atoms of each column seem to be displaced, because the intensity of the displaced atomic column is enough. The reason of the displacements of the Au columns is not clear. The first possibility is the disordered configuration of the CeO_2 side. The intensity of the Ce columns is weakened just below the displaced Au columns, indicating the presence of defects or disordered configuration in that region of CeO_2. The second possibility is the structural fluctuation associated with the movement of atoms enhanced by the electron beam irradiation [13, 14]. Of course, this point may be combined with the first point. In any case, the present results indicate the possibility that disordered configurations tend to be formed near the perimeter of the Au particle, which is important for the catalytic activity and the dynamical structural change of Au/CeO_2 catalysts.

The atomic columns of Au and Ce at the interface are successfully observed by the HAADF-STEM. It is

important to clarify the position of oxygen at the interface in order to investigate the relation between the interface electronic structure and the catalytic activity, because the stoichiometry of oxide surfaces, namely the interface stoichiometry, strongly affects the adhesion and electronic structure of metal/oxide interfaces [19, 21]. It is difficult to observe oxygen columns directly by HAADF-STEM and also by conventional HRTEM. In order to elucidate reasonable interface configurations, it should be effective to perform first-principles calculations of various interface models so as to reproduce the experimentally observed structure and properties.

Conclusion

The Au/CeO_2 model catalyst was prepared and TEM and HAADF-STEM observations were carried out.

1. The growth of Au particles on CeO_2 is suppressed in the reductive condition.
2. The Au/CeO_2 interface was clearly observed by HAADF-STEM, and the positions of Au and Ce atomic columns were directly identified from the image.

Acknowledgements This work was supported by the Japan Society for the Promotion of Science (JSPS-Grant-in-Aid for Scientific Research (B) 18360322). The authors are grateful to Drs. S. Ichikawa (Osaka University), K. Okazaki, and S. Tanaka (AIST) and Prof. M. Haruta (Tokyo Metropolitan University) for their valuable comments and stimulating discussion. The authors are also grateful to Ms. J. Maekawa and Ms. M. Makino for their assistance with sample preparation.

References

1. Haruta M (1997) Catal Today 36:153
2. Haruta M (2003) Chem Rec 3:75
3. Haruta M, Date M (2001) Appl Catal A Gen 222:427
4. Fu Q, Weber A, Flytzani-Stephanopoulos M (2001) Catal Lett 77:87
5. Burch R (2006) Phys Chem Chem Phys 8:5483
6. Sakurai H, Akita T, Tsubota S, Kiuchi M, Haruta M (2005) Appl Catal A Gen 291:179
7. Manzoli M, Boccuzzi F, Chiorino A, Vindigni F, Deng W, Flytzani-Stephanopoulos M (2007) J Catal 245:308
8. Lu JL, Gao HJ, Shaikhutdinov S, Freund HJ (2007) Catal Lett 114:8
9. Spence JCH (1999) Mater Sci Eng R26:1
10. Browning ND, Pennycook SJ (1996) J Phys D Appl Phys 29:1779
11. Pennycook SJ, Boatner LA (1988) Nature 336:565
12. Pennycook SJ, Jesson DE (1991) Ultramicroscopy 37:14
13. Akita T, Okumura M, Tanaka K, Kohyama M, Haruta M (2005) J Mater Sci 40:3101
14. Akita T, Okumura M, Tanaka K, Kohyama M, Haruta M (2006) Catal Today 117:62
15. Akita T, Tanaka K, Kohyama M, Haruta M (2007) Catal Today 122:233
16. Esch F, Fabris S, Zhou L, Montini T, Africh C, Fomasiero P, Comelli G, Rosei R (2005) Science 309:752
17. Leitenburg C, Trovarelli A, Kašpar J (1997) J Catal 166:98
18. Zanella R, Louis C (2005) Catal Today 107–108:768
19. Okazaki K, Morikawa Y, Tanaka S, Tanaka K, Kohyama M (2004) Phys Rev B 69:235404
20. Bernal S, Botana FJ, Calvino JJ, López-Cartes C, Pérez-Omil JA, Rodríguez-Izquierdo JM (1998) Ultramicroscopy 72:135
21. Kohyama M, Tanaka S, Okazaki K, Akita T (2007) Mater Trans 48:675